2016 3rd International Conference on Engineering Technology and Application (ICETA 2016)
ISBN: 978-1-60595-383-0

Optimized Constant Current and Ripple Control of Non-electrolytic Capacitor LED AC/DC Power

Zhongyuan Li, Chunkai Chen*, Shuai Li & Fenglu Zhang
School of Electronic and Information Engineering, Tianjin Polytechnic University, Tianjin, China

ABSTRACT: For the traditional power supply of the non-continuous load Boost-Buck LED, when it has a high power factor, it will produce a significant low frequency ripple current. In this paper, a new type of LED driver power supply technology based on buck boost topology is proposed. The advantage of this technique is that the low frequency ripple current is greatly reduced without affecting the performance of the power factor and the advantages of high efficiency and low cost of the traditional boost buck LED driver are also preserved. We validate the performance of this new technology through a 30W and 50V-2A experimental prototype.

Keywords: large electrolytic capacitor; LED; driving power supply; power factor correction; constant current and constant pressure

1 INTRODUCTION

Light Emitting Diode (LED) has the advantages of energy saving, environmental friendliness, safety and long lifetime. It is the fourth generation light source following incandescent lamp, fluorescent lamp and high-intensity discharge lamp [1-5]. The development of LED lighting technology needs high reliability, high power factor, long lifetime and low cost LED drivers. Lighting LED has the advantages of low power consumption, long life, low environmental impact and high efficiency, which makes the LED technology become more and more popular. In power converter, electrolytic capacitor has lower cost and good performance, which is usually used to stabilize the instantaneous input and output power. However, the service life of electrolytic capacitors is shorter than that of other devices. The study shows that the failure of the electrolytic capacitor is the most common in the LED drive power supply. The life of electrolytic capacitor is usually 5000h/105℃, which has been the bottleneck of the life of the power supply. Therefore, the electrolytic capacitor is very important for ensuring the life of the LED lighting device. Therefore, people put forward a variety of solutions to remove the large size, short life of electrolytic capacitors. But the output of the converter will cause a ripple current of l20Hz, which can be used in parallel LC filter for reducing the l20Hz pulse components. The electrolytic capacitor will not only increase the cost, but also require a number of printed circuit board spaces. The existing techniques include: (1) the input current waveform of the driving power is modulated, and the peak of the input pulse power is reduced by reducing the imbalance of the input and output power; (2) The difference between the input and output power of the large inductor and the larger size of the thin film capacitor is achieved, although the passive energy storage element is of great size and weight; (3) Increasing the ripple and the input current to the three and five harmonics, thereby achieving the purpose of removing the electrolytic capacitor [6-10].

These methods are to improve the existing control or power circuit, which can be divided into two categories: one is to retain the original topology, and the control method is improved; the other one is to construct a new circuit topology. In order to achieve the power factor correction and DC-DC conversion, the removal of the low frequency of the low frequency generation in the single stage power supply is proposed. Large capacity energy storage capacitor is replaced by a bidirectional converter. The disadvantage of this scheme is that the output energy is converted to the output three times. And the design of the balance between the power factor and the required output capacitor is presented. However, the scheme is based on

*Corresponding author: chenckoffice@163.com

the sacrifice of the input current harmonics and power factor performance to achieve the goal [11]. In the literature [3], the single stage topology is used in the output stage; the AC component of the PFC converter is absorbed by the bidirectional buck boost circuit in the output stage. The switching technology is realized by using multiple fast recovery diodes in the power supply circuit. Literature [6-7] technology is used to discuss the PFC technology. The PFC switch is required to handle the PFC inductor current and LED current. AC-DC LED driver converts a commercial AC voltage to a steady DC voltage and produce constant current for driving LED. Electrolytic capacitor should be removed to improve the lifetime and reliability of the LED driver. Our paper is dedicated to the design of a two-stage electrolytic capacitor-less AC-DC LED driver [12-13]. The boost PFC converter is operated in critical current mode, so that the power switch achieves zero-current-switching and the reverse recovery of the boost diode is avoided. The half-bridge series resonant converter is chosen as the DC-DC converter, and it is operated in discontinuous current mode. Such operation not only achieves ZCS for the power switches and rectifier diodes, but also exhibit the characteristic of constant output current, which is deem for driving LED. The operating principle of the two-stage electrolytic capacitor-less AC-DC LED driver is analyzed in details, the parameter design of the power stage is discussed, and the control strategy of it is also presented. A 30W prototype has been built and tested in the lab, and the experimental results verify the effectiveness of the proposed two-stage non-electrolytic capacitor AC-DC LED driver.

2 OPERATING PRINCIPLE

2.1 *Circuit Structure and Principle*

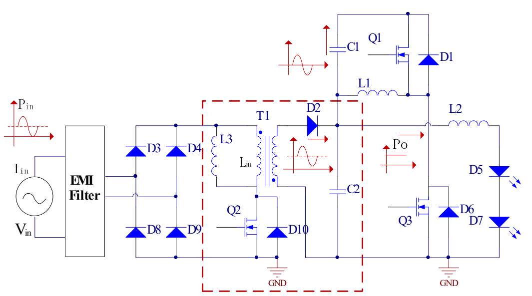

Figure 1. LED AC-DC driver circuit without electrolytic capacitor.

As shown in Figure 1, the switch Q2 enables the flyback converter to work in the DCM mode to achieve the function of the PFC; Q1 and Q3 complement each other. The L1 and C1 are used as the storage device of the bidirectional buck boost converter, while the L2 and C2 constitute the high frequency filter of the output current. Where Lm is the primary winding side inductance, which is the key part of the circuit, it has two main functions: (1) It is a part of the feedback to the DC bus capacitor to reduce the ripple suppression capacitor; (2) A high frequency pulse current is provided in the output of LED. When the input power Pin is less than the output power Po, the operating principle can be divided into four states. When the input power Pin is higher than the output power Po, the operating principle of the Pin is similar to that of the input power Po except for the current counter flow direction.

Let the input voltage is [14]

$$v_{in}(t) = V_{in} \sin \omega_{in} t \tag{1}$$

In the formula (1), v_{in} is the AC input voltage amplitude; ω_{in} is the angular frequency of the AC input voltage. When the input power factor is 1, the instantaneous input power is shown in the formula (2).

$$p_{in}(t) = v_{in} i_{in}(t) = V_{in} I_{in} (1 - \cos 2\omega_{in} t) / 2 \tag{2}$$

Assuming the efficiency of the PFC converter is 100%, the instantaneous input and output power are equal. Because of the constant voltage load characteristics of LED, the output voltage V_o is basically constant, then the PFC output current is

$$i_o(t) = V_{in} I_{in} / (2V_o)(1 - \cos 2\omega_{in} t) = I_o (1 - \cos 2\omega_{in} t) \tag{3}$$

As shown in Figure 2, in one switching period, the converter has four switching modes, and the working conditions are described as follows.

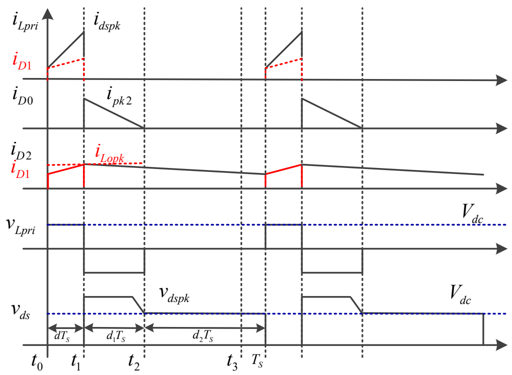

Figure 2. Steady-state operating waveforms.

(1) State 1 [t_0-t_1]: when $t=t_0$, open Q2 and Q3, close Q1, the input energy Vin is stored in Lm, and then C_O release energy to L_B and LED, The state ends when the Q2 is closes at $t=t_1$.

(2) State 2 [t_1-t_2]: When $t=t_1$, the Q2 is closed, the Q3 is maintained, and the Q1 is turned off, and

the Q3 is turned on, The energy stored in the Lm is released to Co, L_B, and LED, which ends when the Lm is complete at $t=t_2$.

(3) State 3 [t_2-t_3]: When $t=t_2$, the Q3 is maintained, the Q1 and Q2 are switched off, the Co is released to L_B and LED, which ends when the Q3 is closed and the Q2 is opened $t=t_3$.

(4) State 4 [t_3-t_4]: When $t=t_3$, the Q3 is maintained, the Q2 and Q1 are switched off, the Co is released to L_B and LED, which ends when the Q3 is closed and the Q1 is opened $t=t_4$.

2.2 *Realization method of non-electrolytic capacitor*

When the single stage power supply has achieved a high power factor, there is a balance between the input and the output of the LED power supply. As shown in Figure 3, in order to adapt to the difference of the energy, a large capacity capacitor is indispensable, and the life of electrolytic capacitor greatly limits the service life of LED power supply, so it is very important to eliminate electrolytic capacitor[15].

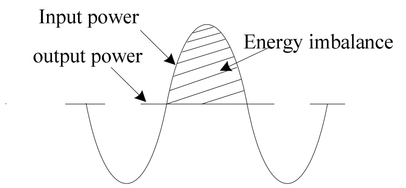

Figure 3. Input and output power waveforms.

Figure 3 shows the imbalance between the two sides of the input and output side of the power supply in half cycle [16]. This energy imbalance is shown by the low frequency ripple current at the PFC output. LED power supply is almost all of the energy output by V_{o1}. The relationship between energy imbalance and voltage fluctuations can be represented by (4):

$$E_{imbalance} = \frac{1}{2}CV_{o1\_\max}^2 - \frac{1}{2}CV_{o1\_\min}^2 = \frac{1}{2}C\left(V_{o1\_\max} + V_{o1\_\min}\right)\left(V_{o1\_\max} - V_{o1\_\min}\right) \tag{4}$$

In the formula (4), the $E_{imbalance}$ is the energy of the half cycle. $V_{o1\_\max}$ represents the maximum value of the V_{o1} within a half cycle, and the $V_{o1\_\min}$ represents the minimum value of the V_{o1} in half cycle. C is the output capacitor of V_{o1}. The capacitor used to complete a certain voltage output voltage can be represented by (5).

$$C = \frac{E_{imbalance}}{\frac{\left(V_{o1} + V_{o2}\right)}{2}\left(V_{o1} - V_{o2}\right)} \tag{5}$$

For a power supply, its output power is 10W, and $E_{imbalance}$ is 0.0273J at the 60Hz line frequency. V_{o1} is allowed by a low frequency ripple voltage of $9V_{P\text{-}P}$, so the required output capacitor can be less than 55uF. The capacitor can be used instead of electrolytic capacitor. In the previous experiments, three 20uf ceramic capacitors can be used instead, and connect to the output voltage V_{o1}.

3 INPUT CURRENT ANALYSIS AND CIRCUIT CHARACTERISTICS

At the input of the circuit end, the PFC is controlled by the Lm in the discontinuous mode (DCM). Basic, the current through the diode D2 will change with the DC bus voltage V_{dc} envelope. V_p and f_L are used to represent the input voltage peak and line frequency, then the corrected voltage is represented by the formula (6). Partial duty cycle d of the discharge is given by (7).

$$v_r = V_p\left|\sin(2\pi f_L t)\right| \tag{6}$$

$$d = \frac{i_{pk,2}L_{\sec}}{V_{dc} - v_r} \tag{7}$$

The average current which pass through D2 is given by (8), i_{pk} is given by (9). The average input current can be given by (10), which indicates that the shape of the input current is affected by the ratio of V_{dc} and V_p. As V_{dc} approaches V_p, the output current becomes more distorted[17].

$$i_{Do,avg} = \frac{i_{pk2}}{2}d_1 = \frac{i_{pk2}}{2}\left(\frac{i_{pk2}L_{\sec}}{V_{dc} - V_p\left|\sin\left(2\pi f_L t\right)\right|}\right) \tag{8}$$

$$i_{pk2} = \left(i_{ds,pk} - \frac{n_3}{n_1}i_{Lo,pk}\right)\frac{n_1}{n_2} \tag{9}$$

$$i_{s,avg} = \frac{L_{\sec}\left(i_{ds,pk} - \frac{n_3}{n_1}i_{Lo,pk}\right)^2\left(\frac{n_1}{n_2}\right)^2}{2V_{dc}\left[1 - \frac{V_p}{V_{dc}}\left|\sin\left(2\pi f_L t\right)\right|\right]} \tag{10}$$

$$v_{ds,pk} = v_{dc}\left(1 + \frac{n_1}{n_2}\right) \tag{11}$$

By the formula (11), the field effect tube voltage is a function of V_{dc} and the conversion ratio (n_2/n_1). The waveform of the input current is a function of V_{dc}. As shown in Figure 4, when the increase of n_2/n_1, $v_{ds,pk}$ is reduced, when the V_{dc} is close to the V_p, n_2/n_1 value and the ratio of V_{dc} and V_p are needed to choose suitable. In Figure 1, the C_2 is the energy storage capacitor, the capacitor C_1 is a high frequency filter capacitor.

Due to C_2 is shifted to the high side, therefore, because of the high input impedance of the first stage converter and the energy exchange between Lsec and C_2, C_2 need energy can is greatly reduced. Therefore, you can use small values of the capacitor C_2, allowing film capacitor as the energy storage capacitor.

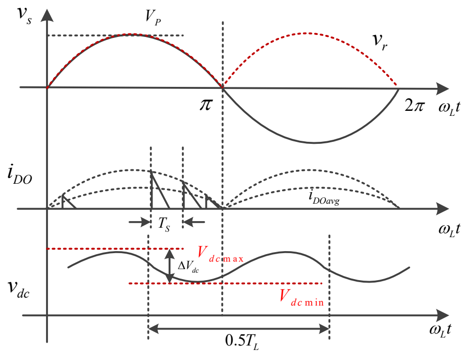

Figure 4. Voltage v_{dc} analysis.

$$\Delta E = \frac{1}{2} C_d \left(V_{dc,\max}^2 - V_{dc,\min}^2 \right) \quad (12)$$

$$\Delta E = \frac{P_{i,avg}}{4\pi f_L} \quad (13)$$

$$C_B = \frac{P_{o,avg}}{\eta 4\pi f_L V_{dc} \Delta V_{dc}} \quad (14)$$

$$L_{o,\min} = \frac{dT_S \left(V_{dc} \frac{n_3}{n_1} - v_o \right)}{2 i_{o,avg}} \quad (15)$$

In the design of the output of the circuit, in order to ensure that the CCM is provided in the i_{Lo}, the minimum value of i_{Lo} can be calculated by (15), and i_{Lo} is the average output current.

4 PARAMETER DESIGN OF THE CONVERTER MAIN CIRCUIT

4.1 *The choice of main components*

The input voltage of diode rectifier bridge should be:

$$V_{rb} = \sqrt{2} \cdot V_{in\_rms\_\max} = \sqrt{2} \times 264 = 373\ (\mathrm{V}) \quad (16)$$

the current:

$$I_{in\_rms\_\max} = \frac{Pin}{\eta \cdot V_{in\_rms\_\min}} = \frac{60}{80\% \times 198} = 0.38\,(\mathrm{A}) \quad (17)$$

The KBP206 (V_R= 600V, I_{FAV}=2A) is set in consideration of the allowance. The peak current of switch is:

$$I_{Qb\_pk\_\max} = \frac{2\sqrt{2} \cdot P_o}{\eta \cdot V_{in\_rms\_\min}} = \frac{2\sqrt{2} \times 60}{80\% \times 198} = 1.07(\mathrm{A})$$

(18)

When the capacitor increases the ripple of energy storage capacitor, the average voltage value is 400V and the ripple voltage ranges from 338V to 460V. CBB capacitors are chosen which pressure value is 630V and the value is 1uF:

The value of $I_{Db\_pk\_\max}$ has been calculated as the formula $I_{Qb\_rms\_\max} = 0.259A$. By the analysis above, it can be known that the voltage stress of Db is 460V, which is considered to be a choice as an energy storage capacitor. Considering the margin, we can choose MUR460($V_R = 460V$, $I_{FAV} = 4A$).

4.2 *Inductance design*

We selected the RM10 type magnetic core, its effective magnetic area is A_e= 96.6mm^2, the window area A_w = 69.53mm^2, the magnetic core material is PC40. The saturation magnetic flux density is B_S= 0.39T at the temperature of 100°C, and ΔB is taken to be ΔB=0.2T. Boost PFC converter works in the current critical continuous mode, then $I_{Lb\_pk\_\max}$ = $I_{Qb\_pk\_\max}$ =1.07A, then the number of L_b turns is:

$$N_{1\_Lb} = \frac{L_b \times I_{Lb\_pk\_\max}}{\Delta B \cdot A_e} = \frac{700 \times 10^{-6} \times 1.07}{0.2 \times 96.6 \times 10^{-6}} = 39.1 \quad (19)$$

On the design of Boost PFC of the system, we choose the L6561 as the most controller chip, which needs an auxiliary winding to measure the voltage across to inductance in order to operate in continuous conduction mode. The inductance L_b whose number of turns of the primary coil is set to about n_{Lb} times that of the secondary coil. The voltage across L_b is v_g and the voltage of A is -v_g/n_{Lb} when Q_b turns on, the voltage across L_b is $v_g - v_{cb}$ and the voltage of A point is $(v_{cb}-v_g)/n_{Lb}$. When the current of inductance is zero, the voltage across L_b is 0 and the voltage of A is 0. When Q_b turns off, the 5th pins of the L6561 measures the voltage of A point is less than 2.1V, the switch will turn on. In order to L6561 can work properly, the inductance L_b whose ratio of the primary coil to the secondary coil should be:

$$\frac{v_{cb}(t) - v_g(t)}{n_{Lb}} > 2.1 \quad (20)$$

By putting the expression of v_{cb} and v_g, it can be calculated that L6561 ratio n_{Lb}=5, the original side turns N_{1_Lb}=40, then the secondary side number of turns is N_{2_Lb} =8.

The air gap of the magnetic columniation is:

$$\delta = \frac{\mu_o . N_{1\_Lb}^2 . A_e}{L_b} = \frac{64\pi \times 10^{-5} \times 96.6}{700 \times 10^{-6}} = 0.28(mm) \quad (21)$$

The μ_o is initial magnetic permeability for air in the expression.

According to the formula (19), the effective value of the inductance current can be calculated to be 0.445A, and the current density of the paper is designed to be J=4A/mm^2, the cross-sectional area of the conductor is 0.111mm^2. We choose four wire windings, considering the auxiliary winding is only used to sample the signal, the current effective value of the flow is very small, the need to use a single wire diameter of the wire wound around the system can be. The filling coefficient of magnetic core K_u is:

$$K_u = \frac{S_w}{A_w} = \frac{\frac{\pi}{4}(1.6N_{1\_Lb} + 0.4N_{2\_Lb})}{A_w} = 0.18 \quad (22)$$

It can be seen from the equation, the winding can be accomplished.

5 EXPERIMENTAL STUDY

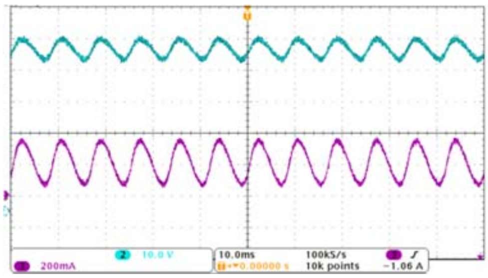

Figure 5. Voltage current value of the power input.

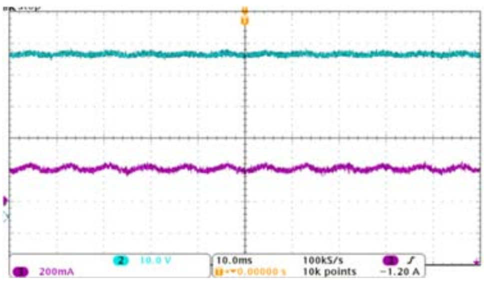

Figure 6. Voltage and current value of the power output.

Figure 5 shows the voltage current value of the power input, and the low frequency elimination of the output voltage between the V_{o1} and output voltage V_{o3} is better in the PFC circuit. The initial ripple of the V_{o1} is determined by the $V_{P\text{-}P}$, after the elimination of the ripple, the ripple voltage on the LED has been reduced to 0.75V. The ripple current and efficiency have been greatly improved compared with the conventional buck-boost LED power supply, and the output capacitor value is greatly reduced. As shown in Figure 6, the conventional buck-boost LED power supply ripple current up to 250mA. In the ripple cancellation technique, the low frequency ripple current has been reduced to 20mA. The ripple rejection rate was about 12.5 times.

6 CONCLUSIONS

In this paper, a simple LED power supply topology with high power factor with a pulse current driving technique is proposed. In the absence of any electrolytic capacitor and complex control method, the single switch circuit in this paper is also capable of reducing the low frequency ripple current. In the proposed topology, a coupled inductor is used to realize the PFC function and provide high frequency ripple current for the output. This paper provides a detailed description of the circuit, working principle and theoretical analysis. Finally, the feasibility of the scheme is demonstrated by a 30W and 50V-2A experimental prototype.

ACKNOWLEDGMENT

The authors gratefully acknowledge financial support from College Student's Innovation and Entrepreneurship Training Program of Tianjin Polytechnic University (Project No: 201510058157).

REFERENCES

[1] B. Wang, X. Ruan, K. Yao, and M. Xu, 2010. A method of reducing the peak-to-average ratio of LED Current for electrolytic capacitor-less AC–DC drivers, *IEEE Trans. Power Electron*., 25(3): 592-601.
[2] S. Wang, Xi. Ruan, K. Yao, S.C. Tan, Y. Yang, and Z. Ye, 2012. A flicker free electrolytic capacitor-less AC–DC LED driver, *IEEE Trans. Power Electron*., 27(11): 4540-4548.
[3] W. Chen and S.Y.R. Hui, 2012. Elimination of an electrolytic capacitor in AC/DC light-emitting diode (LED) driver with high input power factor and constant output current, *IEEE Trans. Power Electron*., 27(3): 1598-1607.
[4] P.S. Almeida, G.M. Soares, D.P. Pinto, and H.A.C. Braga, 2012. Integrated SEPIC buck-boost converter as an off-line LED driver without electrolytic capacitors, In *Proc. IEEE Ann. Conf. IEEE Ind. Electron. Soc*., pp: 4551-4556.
[5] H. Ma, J.S. Lai, Q. Feng, W. Yu, C. Zheng, and Z. Zhao, 2012. A novel valley-fill SEPIC-Derived power supply without electrolytic capacitor for LED lighting application, *IEEE Trans. Power Electron*., 27(6): 3057-3074.
[6] K. Jirasereeamonkul, I. Boonyaroonate, K. Chamnongthai, and M.K. Kazimierczuk, 2005. Application of

power source element in Power-Factor Correction, In *Proc. IEEE TENCON Region*, pp: 1–4.

[7] P.S. Almeida, G.M. Soares, and H.A.C. Braga, 2012. Off-line flyback LED driver with PWM dimming and power factor correction employing a single switch, In *Proc. IEEE/IAS Int. Conf. Ind. Appl*., pp: 1-7.

[8] H. Ma, W. Yu, C. Zheng, J.S. Lai, Q. Feng, and B.Y. Chen, 2011. A universal input high-power-factor PFC pre-regulator without electrolytic capacitor for PWM dimming LED lighting application, In *Proc. Energy Convers. Congr. Expo*., pp: 2288–2295.

[9] M. Ryu, J. Kim, J. Baek, and H.G. Kim, 2012. New multi-channel LEDs driving methods using current transformer in electrolytic capacitor-less AC-DC drivers, In *Proc. IEEE Appl. Power Electron. Conf. Expo*., pp: 2361-2367.

[10] S. Li, S.C. Tan, S.Y.R. Hui, and C.K. Tse, 2013. A review and classification of LED Ballasts, In *Proc. IEEE Energy Convers. Congr. Expo*., pp: 3102-3109.

[11] Q. Hu and R. Zane, 2011. Minimizing required energy storage in Off-Line LED Drivers based on series-input converter modules, *IEEE Trans. Power Electron*., 26(5): 2887-2895.

[12] P. Athalye, M. Harris, and G. Negley, 2012. A two-stage LED driver for high performance high-voltage LED fixtures, In *Proc. IEEE Appl. Power Electron. Conf. Expo*., pp: 2385-2391.

[13] C.A. Cheng, H.L. Cheng, C.H. Chang, F.L. Yang and T.Y. Chung, 2013. A single-stage LED driver for street-lighting applications with interleaving PFC feature, *Next-Generation Electronics (ISNE), 2013 IEEE International Symposium.*

[14] C.A. Cheng, T.Y. Chung, and F.L. Yang. 2013. A single-stage LED driver for street-lighting applications with high PF, *Industrial Electronics (ISIE), 2013 IEEE International Symposium on*.

[15] Y.J. Wang, Y.S. Guan, X.J. Zhang and D.G. Xu, 2013. Single-stage LED driver with low bus voltage, *Electronics Letters*, 49(7): 455-457.

[16] S. Wang, X.B. Ruan, K. Yao, S.C. Tan, Y. Yang and Z.H Ye, 2012. A Flicker-Free Electrolytic Capacitor-Less AC–DC LED Driver. *IEEE Transactions on Power Electronics*, 27(11): 4540-4548.

[17] Q.C. Hu and R. Zane, 2011. Minimizing Required Energy Storage in Off-Line LED Drivers Based on Series-Input Converter Modules. *IEEE Transactions on Power Electronics*, 26(10): 2887-2895.